NSD2 Promotes Tumor Angiogenesis Through Methylating and Activating STAT3 Signaling

Da Song
Huazhong University of Science and Technology
Jingqin Lan
Huazhong University of Science and Technology
Yaqi Chen
Huazhong University of Science and Technology
Anyi Liu
Huazhong University of Science and Technology
Qi Wu
Huazhong University of Science and Technology
Chongchong Zhao
Tsinghua University
Yongdong Feng
Huazhong University of Science and Technology
Jing Wang
Huazhong University of Science and Technology
Xuelai Luo
Huazhong University of Science and Technology
Zhixin Cao
Huazhong University of Science and Technology
Junbo Hu
Huazhong University of Science and Technology
Guihua Wang (ghwang@tjh.tjmu.edu.cn)
GI Cancer Research Institute, Tongji Hospital, Huazhong University of Science and Technology, Wuhan, 430030, China

---

Research

Keywords: NSD2, STAT3, Methylation, Angiogenesis, Post-translational modification

Posted Date: September 8th, 2020

DOI: https://doi.org/10.21203/rs.3.rs-73073/v1

Abstract

Background Tumor angiogenesis plays important roles in tumorigenesis and development, the regulation mechanism of angiogenesis is still not been fully elucidated. Nuclear receptor binding SET domain protein 2 (NSD2), a histone methyltransferase which catalyzes the di-methylation of histone H3 at lysine 36, has been proved a critical molecule in proliferation, metastasis and tumorigenesis. But its role in tumor angiogenesis remains unknown.

Methods Cell Counting Kit 8 (CCK8), scratch assays, transwell-migration assays, tube-formation and mice xenograft model assays were used to confirm the role of NSD2 in the bioprocess of angiogenesis. Bioinformatics analysis, western blot and immunofluorescence staining were used to verify the function of NSD2 in regulating STAT3 signaling pathway. Immunofluorescence co-localization, immunoprecipitation, mass spectrometry and site-directed mutagenesis were performed to determine the NSD2-dependent methylation site of STAT3.

Results: Here we demonstrated that NSD2 promoted tumor angiogenesis *in vitro* and in *vivo*. Furthermore, we confirmed that the angiogenic function of NSD2 was mediated by STAT3. Momentously, we found that NSD2 promoted the methylation of STAT3 and that the inhibition of STAT3 methylation resulted in the attenuation of STAT3 signaling pathway. In addition, mass spectrometry and site-directed mutagenesis assays revealed that NSD2 methylated STAT3 at lysine 163 (K163), and K163 was of significance in the activation of STAT3 signaling pathway.

Conclusion: We conclude that methylation of STAT3 catalyzed by NSD2 promotes the activation of STAT3 pathway and enhances the ability of tumor angiogenesis. Our findings investigate a NSD2 dependent methylation-phosphorylation regulation pattern of STAT3 and reveal that NSD2/STAT3/VEGFA axis might be a potential target for tumor therapy.

Background

Angiogenesis is required in both tumor growth and metastasis and is considered as one of the ten hallmarks of cancer [1]. Because of the rapid proliferation signature of cancer, new blood vessels arise from pre-existing microvasculature to meet the demand of tumor progression [2]. Normally, angiogenesis is strictly under the control of angiogenic and anti-angiogenic factors. However, in some conditions such as inflammation, wound healing, and tumorigenesis, the balance is disrupted and blood vessel formation is promoted [3]. Among the most common factors influencing angiogenesis including VEGF, EGF, HGF, b-FGF, etc, VEGF seems to be the most important molecule [4–6]. VEGF antagonists, such as bevacizumab significantly attenuate angiogenesis and have been used in the treatment of multiple carcinomas [7, 8]. However, similar to most targeted drugs, VEGF antagonists also encounter both primary and secondary resistance, which is associated with the failure of VEGF antagonists [9]. Therefore, an in-depth exploration of the mechanism of tumor angiogenesis as well as its regulation is crucial and may be of great help in guiding the clinical targeted therapy.

Signal Transducers and Activators of Transcription (STATs) are a vital protein family of transcription factors widely studied in cancer research. STAT3 was identified at first as an acute phase response factor activated by the cytokine interleukin-6 (IL-6) [10, 11]. STAT3 plays a key role in several biological processes in carcinoma, including angiogenesis, proliferation, resisting apoptosis, evading the immune response, and so on, and nearly all the hallmarks of cancer proposed by Weinberg are under the regulation of STAT3 [12, 13]. In recent years, non-classical post-translational modifications such as methylation, acetylation, ubiquitination, and SUMOylation, has gained considerable attention in recent years [14]. STAT3 is reported to be methylated by SET9 and EZH2 at different residue sites resulting in different transcription activating status of STAT3 [15–18]. Acetylation of STAT3 catalyzed by acetyltransferase p300 is reported to be essential in the formation of STAT3 homodimer, which is thought to play an important transcription factor function [19].

NSD2 (also known as WHSC1 and MMSET) is a histone methyltransferase catalyzing the demethylation of histone 3 at lysine 36 (H3K36me2) and is associated with active transcription of a series of genes [20]. NSD2 plays a significant role in cell development, and NSD2 haploinsufficiency is associated with Wolf-Hirschhorn syndrome (WHS) which is a multiple malformation syndrome [21]. Meanwhile, NSD2 knocked-out mice exhibited embryonic development disorder [22]. In recent years, the function of NSD2 in all cancer types have been gradually revealed. Multiple myeloma (MM), one of the most fatal hematologic malignancies, is often characterized by chromosomal translocation [23]. Among them, the t (4;14) translocation, which is one of the major types of chromosomal translocation in MM, is associated with the overexpression of NSD2 and leads to a poor prognosis [24–26]. NSD2 is overexpressed in prostate cancer, especially in metastatic niche and has been proven to be associated with the poor prognosis in prostate cancer patients [26], NSD2 can also directly methylate PTEN and enhance the DNA damage repair ability in colorectal cancer, and as a result, enhance the resistance of cancer cells to chemotherapy [27]. Similar results have been reported in other solid carcinomas such as esophagus carcinoma, stomach carcinoma, hepatocellular carcinoma, lung cancer, corpus uteri malignancy, etc [28]. However, the function of NSD2 in angiogenesis remains to be explored.

Here, we demonstrated NSD2 interacted with STAT3 enhancing its methylation and phosphorylation and resulting in transcription activation of VEGFA and promotion of angiogenesis. Moreover, this study identified Lysine 163 (K163) of STAT3 as the NSD2-dependent methylation site, and this residue could be of significance in the activation process of STAT3 signaling pathway. The findings indicate that NSD2 plays a vital role in angiogenesis and could be a potential therapeutic targeted for tumor angiogenesis.

Methods

Cell culture and Reagents

SW48, SW480, LoVo, and HUVECs were all purchased from the American Type Culture Collection (Manassas, VA, USA) and cultured in Dulbecco's modified Eagle's medium (Gibco BRL, Grand Island, NY) supplemented with 10% fetal bovine serum (Gibco BRL) and 1% penicillin/streptomycin in a humidified

incubator with 5% CO2 at 37 ℃. Antibodies against Histone 3 (#4499), Flag (#14793), STAT3 (#9139), Tri-Methyl Lysine Motif (#14680). Di-Methyl Lysine Motif (#14117), Mono Methyl Lysine Motif (#14679), and phospho-Stat3 (Tyr705) (#9145) were purchased from Cell Signaling Technology (Danvers, MA, USA). Antibodies against GAPDH (sc-137179), NSD2 (sc-365627), and HA (sc-7392) were purchased from SantaCruz Biotechnology (Santa Cruz, CA, USA). Antibody against VEGFA (A5708) was purchased from Abclonal Technology (Wuhan, China).

Stable cell lines and plasmid construction

Lentiviral vectors containing shNC (negative control, NC) and shRNA-NSD2 were constructed using the vector PLKO.1. The full-length NSD2 with HA-tag was cloned into a lentiviral vector PLKO.AS3w which was used for overexpressing stable cell lines. The full-length STAT3 with Flag-tag was cloned into the pcDNA3,1(+) vector. Full-length STAT3 was divided into three parts, and the three fragment plasmids were constructed. STAT3 K163R and STAT3 K244R were generated using a Mut Express II Fast Mutagenesis Kit V2 (Vazyme, Nanjing, China). All the primers used are listed in Table S1.

Cell Counting Kit-8 (CCK8) assay

HUVECs (2.5×10^3/100 μl) were seeded into 96-well plates and treated with CM from altered disposed cell lines. At the indicated times (0 h, 24 h, 48 h and 72 h), 10 μl of CCK was added to the medium. Following incubation for 2 h, the cell proliferation rate was assessed by measuring the absorbance at 450nm of the medium.

Cell migration assay

HUVECs (5×10^4/200 μl) were suspended using medium without serum. The cells were then seeded into the upper chamber of a transwell chamber, and 650 μl of CM from different disposed CRC cells was added to the lower chamber. The cells were incubated for 16 h and stained with a violet solution. Images were captured using a light microscope.

Wound healing assay

HUVECs were seeded into 6-well plates. When 98% of cell density was reached, the media were replaced with CM from altered cells including 1μM 5-fluouracil to block the proliferation after scratch wound, and a 200 μl sterile plastic pipette tip was used to scratch the cells. The wound distances were measured using a light microscope. Within 24 h, the wound healing distances were photographed and measured.

Tube formation assay

Growth factor-reduced matrigel (BD Biosciences, NJ, USA). was placed into 96-microwell plates 50μL per well and solidified at 37 °C for 30 min. Then, 4 × 104 HUVECs were separately suspended in CM from different cells and seeded into the pre-coated matrigel microwells. They were incubated for 8 h afterwhich tube formation was observed using an inverted microscope (Eclipse model TS100; Nikon, Tokyo, Japan).

The tube formation ability of the HUVECs was assessed by counting the number of branch points per field.

Immunofluorescence assay

Cells expressing shNC and shNSD2 were seeded on coverslips. The cells were fixed with neutral tissue fixator and washed with PBS three times. The fixed cells were permeabilized with 0.1% Triton X-100 for 2 min, blocked with 1% bovine serum albumin for 1 h, and treated with the indicated primary antibodies at 4OC overnight. The cells were then treated with secondary antibodies and incubated for 1 h and DAPI for 15 minutes at room temperature. Visualization of the cells was done using a confocal laser scanning microscope (Olympus FLUOVIEW FV1000).

Enzyme-linked immunosorbent assay (Elisa)

Secretory VEGFA levels were measured using ELISA (#RK00023, Abclonal Technology, Wuhan, China) kits according to the protocols.

Western blot

Protein samples from tissues and cells were electrophoretically separated by SDS-PAGE and transferred to PVDF membranes (Millipore, MO, USA). Molecular weight specific bands were incubated with their corresponding primary antibodies at 4 °C overnight and were then incubated with HRP-conjugated secondary antibodies for 2 h at room temperature. The bands were visualized with ECL reagents (Thermo Fisher, MA, USA).

Immunoprecipitation (IP) and quantified immunoprecipitation (qIP) assay

Cells were harvested and lysed in NP40 lysis buffer for 30 min. Supernatants were precleared with 10 µl of Protein A/G Magnetic Beads (#HY-K0202, MCE, NJ, USA) for 2 h. For the endogenous IP assay, 3-5 µL antibodies against NSD2 or STAT3 were added into 40 µL magnetic beads that had been resuspended in 500 µL NP40 lysis buffer. The mixture was incubated at 4 ℃ overnight. The magnetic beads were isolated from the mixture, protein supernatants were added to them, and incubated at 4 ℃ for 4 h. For exogenous IP or qIP, Anti-flag or Anti-HA magnetic beads (#B26101 and #26201, Bimake, TX, USA) were used to enrich HA-taged or Flag-taged proteins. The magnetic beads and protein supernatants were incubated for 4 h at 4℃. The beads were then boiled with an SDS-loading buffer. The protein samples were used for the western blot assay.

Quantitative Real-time PCR (qRT-PCR)

Total RNA was extracted using RNAiso (Takara, Japan) according to the manufacturer's instructions. Synthesis of cDNA was done using ABScript II RT Master Mix (RK20403, Abclonal Technology, Wuhan, China). Quantification of the mRNA for the indicated genes was done using an ABI 7300 QuantStudio3 PCR (RT-PCR) System using Genious 2X SYBR Green Fast qPCR Mix (RK21206, Abclonal Technology,

Wuhan, China). Gene-specific primer sequences were designed from the PrimerBank database (Table S1) [29].

Mouse tumor xenograft model

Six-week-old male BALB/c nude mice were purchased from Huafukang Bio-Technology (Beijing, China). Eighteen mice were randomly grouped into three groups. The mice were subcutaneously injected with 5×10^5 SW480 cells expressing shNC and shNSD2. At 8 days post injection, the tumor volume was examined after every 4 days. After 28 days, mice were sacrificed for subsequent experiments. Similarly, 5×10^5 LoVo cells expressing Vector and NSD2 were injected subcutaneously on the mice. At 8 days post injection, the tumor volume was examined every 4 days, meanwhile vehicle or STATTIC was intra tumor injected every two days. After 24 days, mice were sacrificed for subsequent experiments. The animal experiments were performed according to the NIH Guide for the Care and Use of Laboratory Animals with the approval of the Institutional Animal Care and Use Committee at Tongji Hospital.

Modification residue identification by mass spectrometry detection

The STAT3 protein sample enriched by the IP assay was separated by SDS-PAGE. After Coomassie bright blue staining, the gel band of interest was excised and sent to the National Protein Science Facility, School of Life Science, Tsinghua University. The gel band was digested, dried, and redisolved in 0.1% trifluoroacetic acid. Peptides were analyzed by an Orbitrap Fusion mass spectrometer.

The MS data was searched against the target protein database from UniProt using an in-house Proteome Discoverer (Version PD1.4, Thermo-Fisher Scientific, USA). The search criteria were: full trypsin specificity was required; carbamidomethylation (C) were set as the fixed modifications; the oxidation (M) and methyl (K/R) were set as the variable modification; precursor ion mass tolerances were set at 20 ppm for all MS acquired in an orbitrap mass analyzer; and the fragment ion mass tolerance was set at 0.02 Da for all MS2 spectra acquired.

Statistical analysis

All data were analysed with GraphPad Prism 7.0 (LaJolla, CA, USA). Two-tailed Student's t-tests and ANOVA analysis were used. Statistical significance was set at $p < 0.05$.

Results

Inhibition of NSD2 moderates tumor-induced angiogenesis *in vitro*

NSD2 has been reported to promote proliferation, chemotherapy-resistance, migration, and invasion in altered malignancies. However, until now, little has been revealed about the role of NSD2 in tumor angiogenesis. Since NSD2 is reported to be up-regulated and predicts poor prognosis in varieties of carcinomas, and angiogenesis plays an important role in tumor progression, the relationship between NSD2 and tumor-induced angiogenesis requires to be explored. In this study, we performed a GSEA

analysis using publically available datasets and found that the up-regulation of NSD2 was related to the bioprocess of angiogenesis (Fig.1A). To detect the function of NSD2, we constructed stable NSD2 shRNA-NSD2(shNSD2)-expressing SW48 and SW480 cell lines using two lentiviruses containing two altered shRNA sequences against NSD2 (Fig.1B). A CCK8 assay was performed to evaluate the proliferation ability in human umbilical vein endothelial cells (HUVECs) incubated with different condition medium (CM). The proliferative ability of HUVECs was found to be moderate in cells expressing shNSD2 compared with those expressing shRNA-NC (shNC) (Fig.1C and 1D). Besides, the proliferation and migration of HUVECs were found to be vital for angiogenesis. Therefore, a scratch assay was performed to evaluate the migration ability of HUVECs, and the results showed that CM from shNSD2 cells inhibited the migratory ability of HUVECs (Fig. S1A, S1B, S1C and S1D). As expected, in a transwell-migration assay, similar results were obtained showing that CM from shNSD2 cells significantly attenuated HUVECs migration compared with CM from shNC cells (Fig.1E, 1F and 1G). A tube formation assay was performed using HUVECS incubated with CM as mentioned above. Less tube formation was observed in the shNSD2 groups compared with the shNC groups (Fig.1H, 1I and 1J). In conclusion, NSD2 attenuates tumor-induced angiogenesis *in vitro*.

Loss of NSD2 attenuates the expression of VEGFA and inhibits angiogenesis *in vivo*

Studies reveal that a series of angiogenic factors are involved in tumor-induced angiogenesis. In this study, we showed that NSD2 could promote tumor angiogenesis, therefore we further investigated if NSD2 could influence the spectrum of angiogenic factors. To verify this hypothesis, we detected the mRNA expression level of several angiogenic factors such as VEGFA, PDGFB, etc. with the intervention of NSD2. Loss of NSD2 was found to inhibit the expression of VEGFA (Fig.2A). Besides mRNA expression, NSD2 also influenced the expression of VEGFA protein (Fig.2B). As an angiogenic factor, only secretory VEGFA could promote angiogenesis in the tumor microenvironment (TME). Therefore, it was important to investigate whether NSD2 influenced the secretion of VEGFA. As expected, the ELISA assay revealed that NSD2 knockdown decreased the levels of secretory VEGFA in CM (Fig.2C and 2D).

To confirm the function of NSD2 in promoting angiogenesis and upregulating VEGFA, a mouse xenograft model was set up using shNC and shNSD2 SW480 cell lines. After 28 days, mice were sacrificed and the xenografts gathered. Xenografts formed by shNSD2 cells were smaller in appearance compared with those formed by shNC cells (Fig.2E). After tumors became visible to naked eyes, tumor volumes were calculated every 4 days and a tumor growth curve is drawn, which indicated that tumors in the shNSD2 group grew slowly compared with the shNC group (Fig.2F). After the xenografts were collected, we measured the weight of these xenografts and found that xenografts formed using NSD2 downregulated cells were lighter in weight (Fig.2G). Besides, the protein expression of NSD2 and VEGFA of the xenograft was detected using western blot assay, and the results showed that the loss of NSD2 attenuated the expression of VEGFA *in vivo* (Fig.2H). Consistent with the above results, IHC staining was performed and revealed that knockdown of NSD2 inhibited the expression of VEGFA (Fig3.I). IHC staining results of CD31, which was considered one of the major markers of vascular endothelial cells, revealed

that tumor vessel density decreased with NSD2 intervention (Fig.2J). These findings indicate that loss of NSD2 inhibits angiogenesis by downregulating expression of VEGFA *in vivo*.

NSD2 influences the activation of the STAT3 signaling pathway

INCB054329, a bromodomain and extraterminal domain (BET) inhibitor, could be regarded as a potent inhibitor of NSD2 and was reported to suppress the JAK-STAT pathway [30]. Meanwhile, GSEA analysis was performed in two different GEO datasets and results showed that the up-regulation of NSD2 was significantly associated with the IL-6/STAT3 pathway (Fig.3A and 3B). Therefore, we put forward the hypothesis that NSD2 activates the STAT3 signaling pathway to up-regulate the expression of VEGFA promoting tumor angiogenesis. To test this hypothesis, we detected the phosphorylation and total levels of STAT3 in multiple cell lines. Western blot analysis revealed inhibition of NSD2 could impair the phosphorylation of STAT3, while overexpression of NSD2 led to an increase in STAT3 phosphorylation (Fig.3C and 3D). STAT3 functions as a transcription factor, hence, the nuclear translocation extent of STAT3 can reflect its functional status to some extent. The subcellular location of STAT3 upon the intervention of NSD2 was detected, and results showed that NSD2 knockdown resulted in the translocation of STAT3 from the nucleus to the cytosol (Fig.3E). Conversely, the overexpression of NSD2 promoted STAT3 translocation from the cytosol to the nucleus (Fig.3F). Consistently, an immunofluorescence assay was performed, and as expected, when the expression of NSD2 was attenuated, the aggregation of STAT in the nucleus also decreased (Fig.3G). Taken together, NSD2 influenced the activation of the STAT3 signaling pathway.

The angiogenic function of NSD2 is mediated by STAT3 signaling pathway

STAT3 signaling pathway plays a vital role in the regulation of VEGFA secretion and angiogenesis under physiological and pathological conditions. In this study, we proved that NSD2 promoted angiogenesis, VEGFA expression, and upregulation of the STAT3 signaling pathway. We then determined if the function of NSD2 was dependent on the STAT3 signaling pathway. NSD2 was overexpressed with or without STAT3 knockdown and the phosphorylation of STAT3 and expression of VEGFA detected by western blot assay. Increased phosphorylation of STAT3 and upregulation of VEGFA were reversed by STAT3 knockdown (Fig.4A and 4B). CCK8 assay was performed to evaluate the proliferative ability of HUVECs incubated with CM from tumor cells. The Result showed that HUVECs incubated with CM from NSD2 overexpressing cells grew faster, but these results were reversed by STAT3 intervention (Fig.4C and 4D). The migration ability of HUVECs incubated with altered CM was measured by stretch and transwell assay. Consistently, HUVECs incubated with CM from NSD2 overexpressing cells exhibited better migratory ability and this effect was inhibited by STAT3 intervention (Fig.4E, 4F, 4G, S2A, S2B, S2C and S2D). Furthermore, the angiogenic effect of CM from cells expressing NSD2 was enhanced as detected by HUVECs tube-formation assay, while the angiogenic function of NSD2 was reversed by attenuating STAT3 expression (Fig.4H, 4I and 4J). Consistent with the above results, ELISA results showed that the concentration of VEGFA in CM was elevated in NSD2 overexpressing cells but was reversed by downregulating STAT3 expression (Fig.S2E and S2F). Taken together, the angiogenic function of NSD2

was reversed by STAT3 intervention. Therefore, we concluded that the angiogenic function of NSD2 is mediated by STAT3 signaling pathway.

STAT3 inhibitor STATTIC abolishes the angiogenic function of NSD2 *in vivo*.

The transcription factor STAT3 plays an important role in oncogenesis and tumor development, hence, targeted drugs against the STAT3 signaling pathway have been widely studied. Early-stage clinical trials have been conducted using STAT3 inhibitors in altered tumors. Here, STATTIC, which is considered an effective STAT3 inhibitor was selected to observe the therapeutic effect in NSD2-overexpressing carcinomas. The effect of STATTIC in the LoVo cell line overexpressing NSD2 was investigated. Surprisingly, NSD2 was found to upregulate the phosphorylation of STAT3 and the expression of VEGFA, and these effects were reversed by the addition of STATTIC (Fig.5A). Next, a xenograft model was set up using LoVo cell line to observe the effect of STATTIC in the NSD2 overexpressing tumor cells xenograft. After 24 days, mice were sacrificed and the xenografts were collected and the tumor volume and weight determined. Xenografts formed by NSD2 overexpressing cells were bigger and the effects were reversed by STATTIC (Fig. 5B). The tumor volume was measured *in vivo*, and a growth curve was drawn to determine the growth status of the xenograft, which showed a consistent result with the above results (Fig. 5C). Determination of the weight of xenografts revealed that xenografts formed by NSD2 overexpressing cells were heavier and this effect was reversed by the addition of STATTIC (Fig.5D). To verify this hypothesis *in vivo*, the xenograft homogenate was obtained and a western blot assay was performed. As shown in Fig. 5E, the results were consistent with the *in vitro* results. IHC assay was performed, and the results showed that phosphorylation of STAT3, expression of VEGFA and CD31-positive cell counts were elevated when NSD2 was overexpressed, however, these were reversed by STATTIC (Fig. 5F). According to CD31 staining status, microvessel density was elevated with NSD2 overexpression and was blocked with the addition of STATTIC (Fig. 5G). Taken together, we concluded that NSD2 promoted tumor proliferation and angiogenesis *in vivo* while these effects were blocked by the use of STAT3 inhibitor STATTIC.

NSD2 directly interacts with and methylates STAT3 to activate the STAT3 signaling pathway

To further investigate the mechanism by which NSD2 regulates the phosphorylation of STAT3, we performed an immunoprecipitation assay in the SW480 cell line and explored the physical interaction between NSD2 and STAT3 endogenously (Fig.6A). Furthermore, we constructed the overexpressing plasmid HA-NSD2 and Flag-STAT3, and both were co-transfected in the HEK293T cell line. An immunoprecipitation assay was performed to verify the exogenous interaction, and a consistent result was obtained (Fig. 6B). To further support this result, immunofluorescence was performed to observe the co-localization status of NSD2 and STAT3 (Fig. 6C). NSD2 is a histone methyltransferase, hence we put forward our hypothesis that NSD2 could methylate STAT3 protein. To confirm this hypothesis, immunoprecipitation was carried out to detect the methylation status of STAT3 with or without NSD2 intervention. We concluded that downregulation of NSD2 resulted in the loss of methylation of STAT3 protein, while overexpression of NSD2 was associated with the hyper-methylation of STAT3 protein (Fig.

6D and 6E). We further tried to explain the relationship between STAT3 methylation and phosphorylation. DZNep, is an inhibitor reported to be global histone methylation rather than an EZH2 inhibitor, was used to confirm the influence of STAT3 methylation upon phosphorylation. Surprisingly, we found that NSD2 upregulated both the phosphorylation and methylation of STAT3, while the addition of DZNep successfully blocked the methylation of STAT3 protein and resulted in a decrease in STAT3 phosphorylation (Fig. 6F). To find out the specific binding domain between NSD2 and STAT3 and the NSD2 dependent methylation residue of STAT3, we constructed three fragment plasmids of STAT3 based on the natural structural domain (Fig. 6G). Next, we overexpressed these fragment plasmids in the HEK293T cell line and performed an immunoprecipitation assay to determine which fragment of STAT3 combined with NSD2. The results showed that Fragment1 (AA1-320) of STAT3 interacted with NSD2 (Fig.6H). These finds indicated that NSD2 interacted with and methylated STAT3 to activate the STAT3 signaling pathway.

Lysine 163 of STAT3 is vital in NSD2 mediating STAT3 methylation and activation In this study, we just proved that NSD2 directly interacted with and methylated STAT3. To find out the NSD2-dependent STAT3 methylation site, immunoprecipitation was used to enrich the STAT3 protein for mass spectrometry. Coomassie blue staining and mass spectrometry results revealed that we successfully gathered enough specific STAT3 protein (Fig. 7A). We identified 14 lysine residues in our spectrometry result (Table S2). Among them, some residues such as K49 and K140 which were already reported to be methylated residues were also observed in mass spectrometry results. Enzyme catalyzed reactions need the interaction between enzymes and substrates. One specific lysine is catalyzed by one specific methyltransferase. Therefore, by analyzing the mass spectrometry result and searching for the lysing residues located in the first fragment of the STAT3 protein and excluding the lysine residues which were already reported to be catalyzed by other enzymes, we have found two possible lysine residues, K163 and K244 as NSD2-dependent methylation sites (Fig. 7B). A secondary mass spectrometry result is shown to prove the K163 methylation status of STAT3 (Fig. 7C). Next, we investigated the target site of the NSD2-dependent STAT3 methylation residue between the two possible sites. We constructed K to R mutant plasmid at K163 and K244 respectively, by overexpressing or downregulating NSD2, and immunoprecipitation used to detect the methylation status of STAT3. The results showed that at first both site mutations attenuated the methylation level of STAT3. The changes in NSD2 expressing level influenced the methylation status of K244R mutant rather than K163R mutant (Fig. 7D and 7E). These results implied that NSD2 influenced the methylation of STAT3 at lysine 163. We also analyzed the conservative property between different species and concluded that 163 of STAT3 is conservative in most species (Fig. S3A). Finally, we performed an IP assay and western blot assay to confirm whether K163 was an important residue for the activation of STAT3, by comparing STAT3 wildtype with STAT3 K163R mutant. The results showed that K163 played an important role in the activation of the STAT3 signaling pathway (Fig. 7F). In conclusion, we proved that NSD2 directly interacted with STAT3 and methylated the latter at K163 residue which played a vital role in the activation of the STAT3 signaling pathway (Fig. 7G).

Discussion

In this study, we confirmed that NSD2 is associated with STAT3 to methylate and change its phosphorylation level. Moreover, we identified K163 as an NSD2-dependent methylation site of STAT3, which is also responsible for the IL-6 mediated STAT3 phosphorylation. Both EZH2 and SET9 are reported to have the ability to methylate STAT3 at different amino residues upon IL-6 stimulation [15, 16]. In this study, NSD2 was found to also take part in this process. Therefore, there is a possibility that not only one methyltransferase or one specific methylation residue is fully responsible for the activation process. This kind of methylation-phosphorylation crosstalk is a common phenomenon in the regulation of all types of signaling pathways, which guarantees the precise regulation of various biological behaviors. In this study, We confirmed another regulatory role of the STAT3 pathway following the methylation-phosphorylation.

Post-translational modification is of great significance in regulating protein activities. As one of the post-translational modifications, methylation has been greatly researched in recent years. Besides research on histones and non-histone methylation has received considerable attention among researchers. The methylation of non-histone protein may be involved in the regulation of the signaling pathway by influencing protein stability, affecting the activities of transcription factors, influencing other post-translational modifications, altering the protein-protein interaction (PPI) and so on [31-33]. For example, AKT was reported to be methylated by SETDB1 at K64 and K140/142 respectively promoting the activity of PI3K/AKT signaling pathway [34, 35]. Even more important, mithramycin, an anti-neoplastic antibiotic is reported to effectively inhibit SETDB1 expression and function, and overcome the resistance of KRAS mutant CRC cells to cetuximab both *in vitro* and *in vivo* [36]. NSD2 is a histone methyltransferase responsible for di-methylation of histone3 at lysine 36 (H3K36me2). NSD2 possesses the capacity to methylate histones, hence could have the ability to methylate non-histone proteins as well. A previous study elucidated that NSD2 methylate PTEN at K349, promoting its phosphorylation by ATM under the DNA double-strand breaks condition and promotes DNA damage repair [27]. In another study, NSD2 was found to methylate Aurora kinase A (AURKA) at K14 and K117 with changes in its kinase activity mediating cell proliferation via the p53 signal pathway [37]. In our study, we identified STAT3 as an original non-histone protein substrate of NSD2 and elucidated the function of a specific methylation amino residue. These findings provided theoretical basis for the usage of potential NSD2 inhibitor and the exploitation of inhibitory peptide to block the interaction between NSD2 and STAT3 and the methylation of specific residue.

Mounting evidence suggests that NSD2 plays a key role in tumorigenesis and tumor progression [38-44]. However, the role of NSD2 in tumor angiogenesis is in distinct. In this study, loss of NSD2 was found to impair colon cancer angiogenesis both *in vitro* and *in vivo*. Angiogenesis is a process controlled by angiogenic and anti-angiogenic factors [3]. Here, we revealed that VEGFA rather than EGF, FGF, HGF, and other factors took part in the NSD2 mediated tumor angiogenesis.

In conclusion, this study has elucidated the function of NSD2 in regulating VEGFA mediated tumor angiogenesis. Mechanistically, we have identified an original methylation amino residue of STAT3 which is dependent on NSD2. Besides, the non-histone protein methylation function of NSD2 in regulating

STAT3 signal pathway transduction is reported. These findings provide evidence that NSD2 antagonists or NSD2-STAT3 interfering peptides can be used as therapeutic targets in targeting angiogenesis.

Conclusion

In summary, our results indicated a methylation-phosphorylation interaction in the process of STAT3 activation, which was mediated by histone methyltransferase NSD2. NSD2 methylates STAT3 on K163, which promotes phosphorylation and nuclear translocation of STAT3, as well as promotes the expression of VEGFA and tumor angiogenesis. Therefore, both NSD2 and K163 methylation of STAT3 could be a potential target for cancer therapy.

Abbreviations

NSD2: nuclear receptor binding SET domain protein 2; STAT3: signal transducer and activator of transcription 3; CM: conditioned medium; HUVEC: human umbilical vein endothelial cell; VEGFA: vascular endothelial growth factor A; EGF: epidermal growth factor; FGF2: fibroblast growth factor 2; HGF: hepatocyte growth factor; PDGFB: platelet derived growth factor subunit B; MVD: microvessel desity.

Declarations

Acknowledgements

We are grateful to the members in Guihua Wang's lab and Junbo Hu's lab for the critical inputs and suggestions.

Authors' contributions

GH.W conceived the project. GH.W and JB.H acquired funding and designed the majority of experiments. ZX.C and XL.L supervised the project and gave some advice. D.S wrote the manuscript and performed most of the molecular biological experiments. JQ.L analyzed the results. YQ.C, AY.L and Q.W performed most of the phenotype experiments. CC.Zhao did the mass spectrometry detection and analysis. YD.F and J.W made their efforts in the bioinformatics analysis.

Funding

This work is supported by NSFC (No. 81922053 GH Wang, No. 81773113 GH Wang, No. 81974432 GH Wang and No. 81874186 JB Hu).

Availability of data and materials

The mass spectrometry proteomics data is uploaded to the ProteomeXchange Consortium (http://proteomecentral.proteomexchange.org).

Ethics approval and consent to participate

The animal experiments were performed according to the NIH Guide for the Care and Use of Laboratory Animals with the approval of the Institutional Animal Care and Use Committee at Tongji Hospital.

Consent for publication

All authors have been in agreement with the publication of this article.

Competing Interests

The authors have declared no competing interests.

References

1. Hanahan D, Weinberg RA. Hallmarks of cancer: the next generation. Cell. 2011;144(5):646–74.
2. Adams RH, Alitalo K. Molecular regulation of angiogenesis and lymphangiogenesis. Nature reviews Molecular cell biology. 2007;8(6):464–78.
3. De Palma M, Biziato D, Petrova TV. Microenvironmental regulation of tumour angiogenesis. Nature reviews Cancer. 2017;17(8):457–74.
4. Canavese M, Ngo DT, Maddern GJ, Hardingham JE, Price TJ, Hauben E. Biology and therapeutic implications of VEGF-A splice isoforms and single-nucleotide polymorphisms in colorectal cancer. International journal of cancer. 2017;140(10):2183–91.
5. Stratman AN, Schwindt AE, Malotte KM, Davis GE. Endothelial-derived PDGF-BB and HB-EGF coordinately regulate pericyte recruitment during vasculogenic tube assembly and stabilization. Blood. 2010;116(22):4720–30.
6. Stratman AN, Davis MJ, Davis GE. VEGF and FGF prime vascular tube morphogenesis and sprouting directed by hematopoietic stem cell cytokines. Blood. 2011;117(14):3709–19.
7. Saltz LB. Bevacizumab in colorectal cancer: it should have worked. The Lancet Oncology. 2016;17(11):1469–70.
8. Smeets D, Miller IS, O'Connor DP, Das S, Moran B, Boeckx B, Gaiser T, Betge J, Barat A, Klinger R, et al. Copy number load predicts outcome of metastatic colorectal cancer patients receiving bevacizumab combination therapy. Nature communications. 2018;9(1):4112.
9. Haibe Y, Kreidieh M, El Hajj H, Khalifeh I, Mukherji D, Temraz S, Shamseddine A. Resistance Mechanisms to Anti-angiogenic Therapies in Cancer. Frontiers in oncology. 2020;10:221.
10. Darnell JE Jr, Kerr IM, Stark GR. Jak-STAT pathways and transcriptional activation in response to IFNs and other extracellular signaling proteins. Science. 1994;264(5164):1415–21.
11. Minami M, Inoue M, Wei S, Takeda K, Matsumoto M, Kishimoto T, Akira S. STAT3 activation is a critical step in gp130-mediated terminal differentiation and growth arrest of a myeloid cell line. Proc Natl Acad Sci USA. 1996;93(9):3963–6.

12. Yu H, Lee H, Herrmann A, Buettner R, Jove R. Revisiting STAT3 signalling in cancer: new and unexpected biological functions. Nature reviews Cancer. 2014;14(11):736–46.
13. Yu H, Jove R. The STATs of cancer–new molecular targets come of age. Nature reviews Cancer. 2004;4(2):97–105.
14. Bharadwaj U, Kasembeli MM, Robinson P, Tweardy DJ. Targeting Janus Kinases and Signal Transducer and Activator of Transcription 3 to Treat Inflammation, Fibrosis, and Cancer: Rationale, Progress, and Caution. Pharmacological reviews. 2020;72(2):486–526.
15. Yang J, Huang J, Dasgupta M, Sears N, Miyagi M, Wang B, Chance MR, Chen X, Du Y, Wang Y, et al. Reversible methylation of promoter-bound STAT3 by histone-modifying enzymes. Proc Natl Acad Sci USA. 2010;107(50):21499–504.
16. Dasgupta M, Dermawan JK, Willard B, Stark GR. STAT3-driven transcription depends upon the dimethylation of K49 by EZH2. Proc Natl Acad Sci USA. 2015;112(13):3985–90.
17. Kim E, Kim M, Woo DH, Shin Y, Shin J, Chang N, Oh YT, Kim H, Rheey J, Nakano I, et al. Phosphorylation of EZH2 activates STAT3 signaling via STAT3 methylation and promotes tumorigenicity of glioblastoma stem-like cells. Cancer cell. 2013;23(6):839–52.
18. Luo J, Wang K, Yeh S, Sun Y, Liang L, Xiao Y, Xu W, Niu Y, Cheng L, Maity SN, et al. LncRNA-p21 alters the antiandrogen enzalutamide-induced prostate cancer neuroendocrine differentiation via modulating the EZH2/STAT3 signaling. Nature communications. 2019;10(1):2571.
19. Yuan ZL, Guan YJ, Chatterjee D, Chin YE. Stat3 dimerization regulated by reversible acetylation of a single lysine residue. Science. 2005;307(5707):269–73.
20. Kuo AJ, Cheung P, Chen K, Zee BM, Kioi M, Lauring J, Xi Y, Park BH, Shi X, Garcia BA, et al. NSD2 links dimethylation of histone H3 at lysine 36 to oncogenic programming. Molecular cell. 2011;44(4):609–20.
21. Stec I, Wright TJ, van Ommen GJ, de Boer PA, van Haeringen A, Moorman AF, Altherr MR, den Dunnen JT. WHSC1, a 90 kb SET domain-containing gene, expressed in early development and homologous to a Drosophila dysmorphy gene maps in the Wolf-Hirschhorn syndrome critical region and is fused to IgH in t(4;14) multiple myeloma. Human molecular genetics. 1998;7(7):1071–82.
22. Nimura K, Ura K, Shiratori H, Ikawa M, Okabe M, Schwartz RJ, Kaneda Y. A histone H3 lysine 36 trimethyltransferase links Nkx2-5 to Wolf-Hirschhorn syndrome. Nature. 2009;460(7252):287–91.
23. Hideshima T, Mitsiades C, Tonon G, Richardson PG, Anderson KC. Understanding multiple myeloma pathogenesis in the bone marrow to identify new therapeutic targets. Nature reviews Cancer. 2007;7(8):585–98.
24. Chesi M, Nardini E, Lim RS, Smith KD, Kuehl WM, Bergsagel PL. The t(4;14) translocation in myeloma dysregulates both FGFR3 and a novel gene, MMSET, resulting in IgH/MMSET hybrid transcripts. Blood. 1998;92(9):3025–34.
25. Keats JJ, Maxwell CA, Taylor BJ, Hendzel MJ, Chesi M, Bergsagel PL, Larratt LM, Mant MJ, Reiman T, Belch AR, et al. Overexpression of transcripts originating from the MMSET locus characterizes all t(4;14)(p16;q32)-positive multiple myeloma patients. Blood. 2005;105(10):4060–9.

26. Foltz SM, Gao Q, Yoon CJ, Sun H, Yao L, Li Y, Jayasinghe RG, Cao S, King J, Kohnen DR, et al. Evolution and structure of clinically relevant gene fusions in multiple myeloma. Nature communications. 2020;11(1):2666.
27. Zhang J, Lee YR, Dang F, Gan W, Menon AV, Katon JM, Hsu CH, Asara JM, Tibarewal P, Leslie NR, et al. PTEN Methylation by NSD2 Controls Cellular Sensitivity to DNA Damage. Cancer discovery. 2019;9(9):1306–23.
28. Hudlebusch HR, Santoni-Rugiu E, Simon R, Ralfkiær E, Rossing HH, Johansen JV, Jørgensen M, Sauter G, Helin K. The histone methyltransferase and putative oncoprotein MMSET is overexpressed in a large variety of human tumors. Clinical cancer research: an official journal of the American Association for Cancer Research. 2011;17(9):2919–33.
29. Wang X, Spandidos A, Wang H, Seed B: **PrimerBank**: **a PCR primer database for quantitative gene expression analysis**, **2012 update**. *Nucleic acids research* 2012, **40**(Database issue):D1144-1149.
30. Stubbs M, Burn T, Sparks R, Maduskuie T, Diamond S, Rupar M, Wen X, Volgina A, Zolotarjova N, Waeltz P, et al: **The Novel Bromodomain and Extraterminal Domain Inhibitor INCB054329 Induces Vulnerabilities in Myeloma Cells That Inform Rational Combination Strategies**. 2019, 25(1):300–311.
31. Biggar KK, Li SS. Non-histone protein methylation as a regulator of cellular signalling and function. Nature reviews Molecular cell biology. 2015;16(1):5–17.
32. Zhang X, Huang Y, Shi X. Emerging roles of lysine methylation on non-histone proteins. Cell Mol Life Sci. 2015;72(22):4257–72.
33. Hamamoto R, Saloura V, Nakamura Y. Critical roles of non-histone protein lysine methylation in human tumorigenesis. Nature reviews Cancer. 2015;15(2):110–24.
34. Wang G, Long J, Gao Y, Zhang W, Han F, Xu C, Sun L, Yang SC, Lan J, Hou Z, et al. SETDB1-mediated methylation of Akt promotes its K63-linked ubiquitination and activation leading to tumorigenesis. Nat Cell Biol. 2019;21(2):214–25.
35. Guo J, Dai X, Laurent B, Zheng N, Gan W, Zhang J, Guo A, Yuan M, Liu P, Asara JM, et al. AKT methylation by SETDB1 promotes AKT kinase activity and oncogenic functions. Nat Cell Biol. 2019;21(2):226–37.
36. Hou Z, Sun L, Xu F, Hu F, Lan J, Song D, Feng Y, Wang J, Luo X, Hu J, et al. Blocking histone methyltransferase SETDB1 inhibits tumorigenesis and enhances cetuximab sensitivity in colorectal cancer. Cancer letters. 2020;487:63–73.
37. Park JW, Chae YC, Kim JY, Oh H, Seo SB. Methylation of Aurora kinase A by MMSET reduces p53 stability and regulates cell proliferation and apoptosis. Oncogene. 2018;37(48):6212–24.
38. Lhoumaud P, Badri S, Rodriguez-Hernaez J, Sakellaropoulos T, Sethia G, Kloetgen A, Cornwell M, Bhattacharyya S, Ay F, Bonneau R, et al. NSD2 overexpression drives clustered chromatin and transcriptional changes in a subset of insulated domains. Nature communications. 2019;10(1):4843.
39. Cheong CM, Mrozik KM, Hewett DR, Bell E, Panagopoulos V, Noll JE, Licht JD, Gronthos S, Zannettino ACW, Vandyke K. Twist-1 is upregulated by NSD2 and contributes to tumour dissemination and an

epithelial-mesenchymal transition-like gene expression signature in t(4;14)-positive multiple myeloma. Cancer letters. 2020;475:99–108.

40. He C, Liu C, Wang L, Sun Y, Jiang Y, Hao Y. Histone methyltransferase NSD2 regulates apoptosis and chemosensitivity in osteosarcoma. Cell death disease. 2019;10(2):65.
41. Wang JJ, Zou JX, Wang H, Duan ZJ, Wang HB, Chen P, Liu PQ, Xu JZ, Chen HW. Histone methyltransferase NSD2 mediates the survival and invasion of triple-negative breast cancer cells via stimulating ADAM9-EGFR-AKT signaling. Acta pharmacologica Sinica. 2019;40(8):1067–75.
42. Aytes A, Giacobbe A, Mitrofanova A, Ruggero K, Cyrta J, Arriaga J, Palomero L, Farran-Matas S, Rubin MA, Shen MM, et al. NSD2 is a conserved driver of metastatic prostate cancer progression. Nature communications. 2018;9(1):5201.
43. Xie Z, Chooi JY, Toh SHM, Yang D, Basri NB, Ho YS, Chng WJ. MMSET I acts as an oncoprotein and regulates GLO1 expression in t(4;14) multiple myeloma cells. Leukemia. 2019;33(3):739–48.
44. Swaroop A, Oyer JA, Will CM, Huang X, Yu W, Troche C, Bulic M, Durham BH, Wen QJ, Crispino JD, et al. An activating mutation of the NSD2 histone methyltransferase drives oncogenic reprogramming in acute lymphocytic leukemia. Oncogene. 2019;38(5):671–86.

Figures

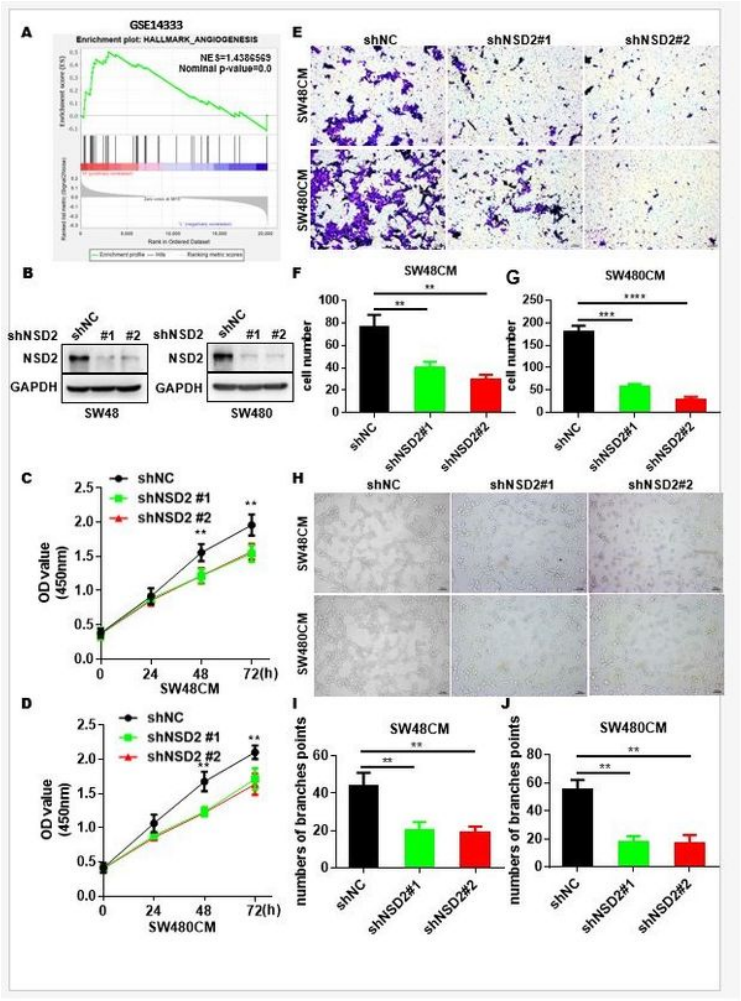

F1. NSD2 promotes angiogenesis in vitro.
A GSEA on angiogenesis bioprocess;B construction of stable knockdown celllines; C condition medium HUVEC CCK8, D/E/F/G tumor CM HUVEC woundhealing and statistics analysis

Figure 1

Inhibition of NSD2 moderates tumor-induced angiogenesis in vitro. A. GSEA analysis showing the relationship between NSD2 expression and the angiogenesis bioprocess; B. Stable NSD2-knockdown cell lines SW48 and SW480 were successfully constructed; C and D. CCK8 assay of HUVECs incubated with CMs from shNC and shNSD2 cells; E, F and G. Transwell-migration assay of HUVECs incubated with identified CMs; H, I and J. Tube-formation assay of HUVECs was performed incubated with identified CMs and the statistical analysis . Results are presented as mean ± SD for n=3, *p <0.05, **p <0.01, ***p <0.001, ****p<0.0001

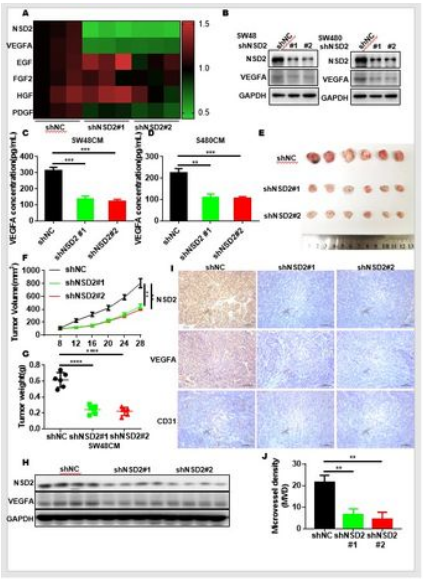

F2. NSD2 promotes the expression of VEGFA and promotes tumor angiogenesis in vivo
A heatmap of results of the expression level changes upon the intervention of NSD2; B .loss of NSD2 attenuates the protein expression level of VEGFA;C/D Elisa assay to estimate the amount of secretory VEGFA in condition medium; E:Xenograft result ;F : tumor weight; G tumor growth

Figure 2

Loss of NSD2 attenuates the expression of VEGFA and inhibits angiogenesis in vivo. A. The qPCR results of shNC and shNSD2 SW480 cells; B. Western blot detecting VEGFA expression upon NSD2 intervention in SW48 and SW480 cell lines; C and D. An ELISA assay detecting VEGFA concentrations in cell medium; E. Mice xenografts formed by SW480 with or without NSD2 intervention, after 28 days, mice were sacrificed and xenografts isolated; F. The growth curve of the tumor volumes; G. tumor weights after sacrificing the mice; H. Western blot results of xenografts homogenates; I. IHC staining of xenografts using antibodies against NSD2, VEGFA and CD31; J. Microvascular densities of the tumors in the three groups as quantified by CD31. Results are presented as mean ± SD for n=3, *p <0.05, **p <0.01, ***p <0.001, ****p<0.0001.

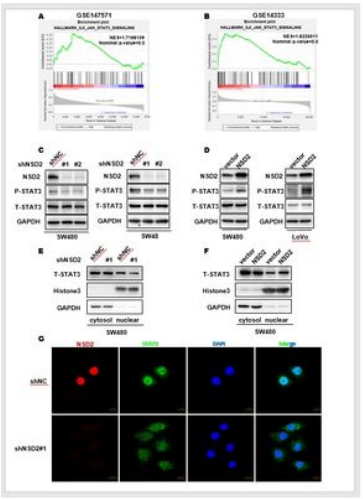

F3. NSD2 influence the activation status of STAT3
A/B GSEA analysis upon IL6/STAT3 pathway ;C loss of NSD2 attenuates the phosphorylation of STAT3;D OE of NSD2 promotes the phosphorylation of STAT3;E loss of NSD2 decreases the nuclear translocation of STAT3;F:OE of NSD2 promotes the translocation of STAT3;G IF assay NSD2 associated with the nuclear translocation of STAT3

Figure 3

NSD2 promotes the STAT3 activation. A and B. GSEA analysis was performed in two different GEO datasets to reveal the association between the expression of NSD2 and the activation of IL-6/JAK/STAT3 pathway. C. Western blot to detect the phosphorylation status changes of STAT3 upon the intervention of NSD2 in SW480 and SW48 cell lines. D. Western blot to detect the STAT3 phosphorylation changes with upregulation of NSD2 in SW480 and LoVo cell lines. E and F. Nuclear and plasma proteins were separated and detected by western blot to detect the subcellular location of STAT3 with intervention or overexpression of NSD2 in SW480 cell line. G. Immunofluorescence assay was performed to reflect the nuclear-location status changes of STAT3 with the intervention of NSD2.

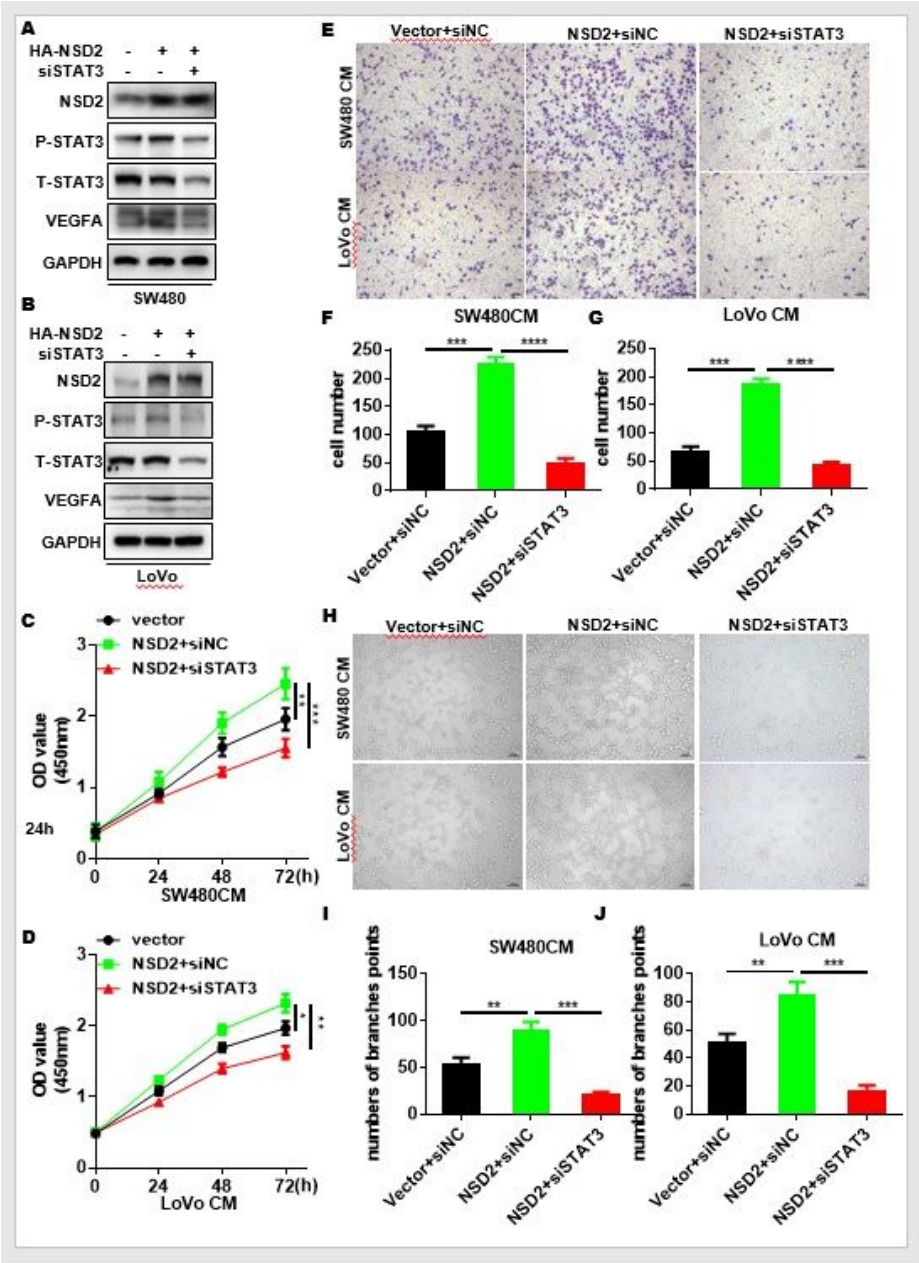

F4. the pro-angiogenesis function of NSD2 is mediated by STAT3.
A/B WB the axix of NSD2/STAT3/VEGFA pathway;C/D CM CCK8 reverse assay;EFGF: CM HUVEC woundhealing assay

Figure 4

The angiogenic function of NSD2 is mediated by STAT3. A and B. Western blot evaluating whether STAT3 was dependent in the NSD2 mediated VEGFA expression promotion by overexpressing NSD2 and silencing STAT3 at the same time. C and D. CCK8 assay assessing the proliferative ability of HUVECs incubated with CMs from cells overexpressed NSD2 and down-regulated STAT3 at the same time. E, F and G. Transwell-migration assay of HUVECs incubated with identified CMs was performed to assess the

migratory ability of HUVECs. H, I and J. Tube-formation assay of HUVECs incubated with identified CMs reflecting the angiogenic function. Results are presented as mean ± SD for n=3, **p <0.01, ***p <0.001, ****p<0.0001.

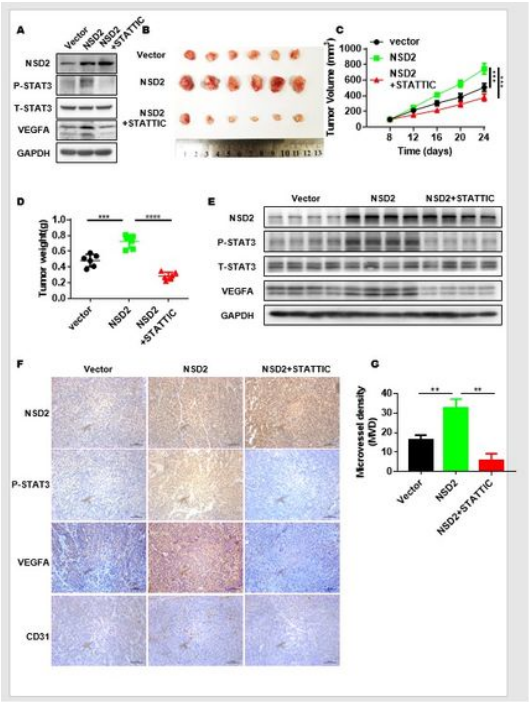

F5. STAT3 inhibitor STATTIC is able to abolish the pro-angiogenesis function of NSD2 in vitro and vivo.
A WB STATTIC reverse the up regulation of VEGFA upon the overexpression of NSD2; B LoVo xenografy plus the application of STATTIC intratumor injection;C tumor weight;D tumor growth; E WB of xenograft F IHC G MVD analysis

Figure 5

STAT3 inhibitor STATTIC abolishes angiogenic function of NSD2 in vivo. A. The effect of STATTIC (10μM, 48 h) was verified in LoVo cells with or without NSD2 overexpression by western blot; B. Xenograft model was set up using vesicle or STATTIC (3.75 mg/kg, every two days) by intratumoral injection after xenografts were touchable, the xenografts were collected ather the mice had been sacrificed; C. Tumor volumes were measured after every 4 days and a growth curve drawn; D. After xenograft collection, the tumor weight was measured; E. Tissue homogenates were obtained from these xenografts and a western blot assay was performed; F and G. IHC staining of xenografts using antibodies against NSD2, p-STAT3, VEGFA and CD31, according to the staining status of CD31, MVD was statistically analyzed.

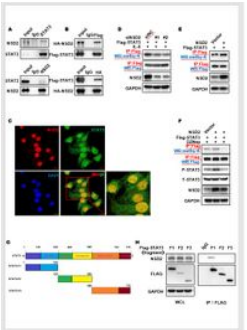

F6 NSD2 could bind and methylate STAT3
AIP endogenous combination; B exogenous IP combination; C IF co-localization;D loss of NSD2 attenuates the methylation and activation of STAT3 ;E OE of NSD2 promotes the methylation and activation of STAT3;F NSD2 mediated the hyper-methylated and hyper-activated status of STAT3 can be blocked by a extensive methylating inhibitor(DZNep);G AND H construction of fragment plasmid of STAT3 NSD2 could interact with first fragment of STAT3

Figure 6

NSD2 directly interacts with and methylates STAT3 to activate the STAT3 signaling pathway A. In SW480 cell line, IP assays using antibodies against NSD2 and STAT3 respectively were performed; B. In HEK293T cell line, after co-transfection of HA-NSD2 and Flag-STAT3, IP assays were performed to enrich HA-NSD2 and Flag-STAT3. C. Immunofluorescence assay was performed to observe the co-localization conditions of STAT3 and NSD2 in SW480 cell line; D and E. Quantified immunoprecipitation assays and western blot to detect the methylation levels of STAT3 with NSD2 upregulation or attenuation; F. Using global methylation inhibitor DZNep ,and a qIP assay was performed to elucidate the methylation and phosphorylation status of STAT3 with NSD2 overexpression and the relationship between these two modifications; G. According to the natural structure of STAT3; the full-length STAT3 was divided into three parts and three fragment plasmids were constructed; H. Using three Flag-tagged fragment plasmids of STAT3 and a IP assay was performed to clarify which domain of STAT3 could bind to NSD2.

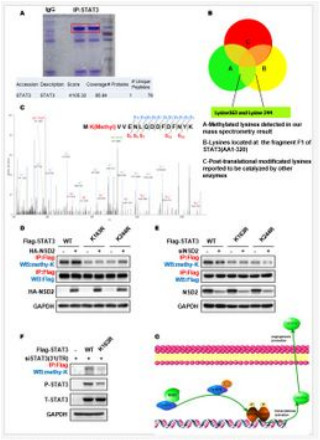

Fig.7 NSD2 methylates STAT3 at K163 promoting the activation of STAT3 signaling pathway.
A. Coomassie brilliant blue staining and mass spectrometry B. strategies for screening specific residue C secondary mass spectrometry result D overexpressing NSD2 and STAT3 mutant E intervention of NSD2 and STAT3 mutant F function of K163 in the activation of STAT3 G idiograph
G. NSD2 binds with the P1 fragment of STAT3; H enrichment of STAT3 protein and authentication with spectrometry) methylation of lysine of STAT3 in our own spectrometry) analysis of our spectrometry result combined with our finding that NSD2 binds with P1-fragment of STAT3, elucidating the K methylation site already reported to be catalyzed by other enzymes ;K the methylation of lysine in STAT3;

Figure 7

Lysine 163 of STAT3 is vital in NSD2 mediating STAT3 methylation and activation A. Using IP assay for the enrichment of STAT3 protein, staining with Coomassie bright blue and verification by mass spectrometry. B. Screening strategy for predicting the possible methylation residues of STAT3 that is dependent on NSD2 function; C. Secondary mass spectrometry result of one possible methylation residue; D and E, qIP assays were performed by detecting the methylation changes of wild type STAT3, K163R and K244R mutants, respectively, with NSD2 overexpression or intervention; F. A siRNA targeting the 3’UTR was used to knockdown endogenous STAT3 and rescued with wild type STAT3 and K163 mutant, after the stimulation of IL-6, the methylation and phosphorylation of STAT3 were detected; G. Schematic diagram of our hypothesis about this project.

Supplementary Files

This is a list of supplementary files associated with this preprint. Click to download.

- TableS2.xlsx
- pageFS3.pptx
- pageFS2.pptx
- pageFS1.pptx
- TableS1.xlsx